Austrian Journal of Earth Sciences | Volume 108/1 | 123 - 138 | Vienna | 2015

How well do pseudosection calculations reproduce simple experiments using natural rocks: an example from high-*P* high-*T* granulites of the Bohemian Massif

Peter TROPPER[1)*)] & Christoph HAUZENBERGER[2)]

DOI: 10.17738/ajes.2015.0008

KEYWORDS

piston cylinder experiments
High-P/high-T granulites
THERIAK-DOMINO
pseudosections
PERPLEX

[1)] Institute of Mineralogy and Petrography, University of Innsbruck, A-6020 Innsbruck, Austria;

[2)] Institute of Earth Sciences, University of Graz, 8010 Graz, Austria;

[*)] Corresponding author, peter.tropper@uibk.ac.at

Abstract

This study represents a comparison between thermodynamic calculations (pseudosections) and the results of the experimental investigation of high-*P*/high-*T* granulites from the Bohemian Massif by Tropper et al. (2005). The experiments were conducted at 750-1000°C at 1.6 GPa, 950°C, 1.4 GPa and 800-900°C at 1.2 GPa in order to model the high-*P*/high-*T* evolution of the south Bohemian granulites. Tropper et al. (2005) used granitic gneiss as starting material whose chemical composition almost perfectly matched the main granulite type of the Southern Bohemian Massif. To test the validity of the experiments pseudosection calculations using the programs THERIAK-DOMINO and PERPLEX were performed in the chemical system K_2O-Na_2O-CaO-FeO-MgO-MnO-Al_2O_3-TiO_2-SiO_2-H_2O (KNCFMMnTiASH). The calculations revealed that the experimentally obtained phase assemblages could very well be reproduced despite the use of different activity models for solid solutions, compositional trends of garnet and feldspars good to satisfactorily. The calculations revealed two major inconsistencies: 1.) the stability of biotite is underestimated in the experiments by ca. 50-100°C and 2.) the amount of melt generated in the experiments is much larger than in the calculations. The reasons for these inconsistencies can be explained by: 1.) electron microprobe analysis of micas from the run products which revealed high F-contents not analyzed previously by Tropper et al. (2005), which is not accounted for in relevant biotite activity models, and by: 2.) the nature of the experimental set-up (lack of eqilibrium in the subsolidus region and fast reaction overstep) which is responsible for generation of abnormously high amounts of melts. Nonetheless the combination of experimental and thermodynamic investigations and its comparison to natural rocks allows gathering deeper insights into the metamorphic evolution of these high-*P*/high-*T* granulites.

Das Ziel dieser Arbeit war der Vergleich zwischen thermodynamischen Berechnungen (Pseudosektionen) und den experimentellen Untersuchungen bezüglich der Genese der Hoch-*T*/Hoch-*P* Granulite aus der Arbeit von Tropper et al. (2005). Die Experimente wurden mit granitischem Ausgangsmaterial bei Temperaturen von 750-1000°C bei 1.6 GPa, bei 950°C und 1.4 GPa und bei 800-900°C bei 1.2 GPa durchgeführt um die *P-T* Entwicklung dieser südböhmischen Granulite im Experiment zu simulieren. Um die Experimente hinsichtlich ihrer Reproduzierbarkeit zu untersuchen wurden Pseudosektionen mittels der Programme THERIAK-DOMINO und PERPLEX im chemischen System K_2O-Na_2O-CaO-FeO-MgO-MnO-Al_2O_3-TiO_2-SiO_2-H_2O (KNCFMMnTiASH) durchgeführt. Die thermodynamischen Berechnungen haben gezeigt dass sich die Mineralparagenesen aus den Experimenten trotz der Verwendung verschiedener Aktivitätsmodelle für die Mischphasen sehr gut und die Mineralzusammensetzungen von Granat und Feldspat gut bis befriedigend reproduzieren lassen. Weiters wurden zwei grosse Inkonsistenzen zwischen den Experimenten und den Berechnungen festgestellt: 1.) die Stabilität von Biotit ist im Experiment ca. 50-100°C höher und 2.) die erzeugte Menge an Schmelze ist in den Experimenten viel höher. Die Erklärungen für diese Abweichungen sind: 1.) in der Untersuchung von Tropper et al. (2005) wurde kein F und Cl in Biotit und Muskovit gemessen wurde und: 2.) das experimentelle Set-up führt durch Ungleichgewicht im Subsolidusbereich und raschem Überschreiten von Schmelzreaktionen zwangsläufig zur Erzeugung hoher Schmelzmengen. Diese Studie zeigt aber trotzdem dass die Kombination von Experimenten und thermodynamischen Berechnungen im Vergleich zu den natürlichen Gesteinen wertvolle Rückschlüsse auf die metamorphe Entwicklung dieser Hoch-*P*/Hoch-*T* Granulite erlaubt.

1. Introduction

The metamorphic evolution of a rock can be deciphered using three approaches: 1.) the practical geothermobarometric approach, 2.) the theoretical approach (phase diagrams, pseudosections, projections) and 3.) the experimental approach. Whereas with the first two approaches it is possible to constrain several stages of the *P-T-X* evolution, the experimental approach allows mostly only the investigation of a distinct *P-T* condition of a rock. On the other hand, experimental investigations allow to put additional constraints on the evolution of a rock under defined *P* and *T* conditions (White et al., 2011). These constraints consider the textural evolution of a given sample as well as additional variables such as aH_2O, nH_2O, fO_2 etc. In order to obtain results as close as possible to the natural rocks it is best to use natural rocks as starting materials. The disadvantage of this method being the complex chemical compositions of the rocks and therefore the deviation from chemical end-member systems (see White et al., 2011). Therefore experiments using natural starting materials need

to be evaluated not only 1.) in terms of their ability to reproduce the natural observations but also 2.) in their ability to be reproduced by thermodynamic calculations (pseudosections). Latter aspect is the aim of this study.

1.1 Partial melting experiments

Experimental studies of partial melting range from chemically simple to complex natural systems (see White et al., 2011). Basically these experiments can be divided into two types depending on the nature of the starting material and the information that can be extracted from the results. While simple chemical systems allow precise determination of thermodynamic paramters of phases involved their chemical systems are too far away from natural rocks and hence the obtained results are oftentimes only of limited use. On the other hand experiments using very large chemical systems, such as natural compositions allow a direct comparison to natural rocks but their ability of extracting thermodynamic data is limited. The main aim of these experiments is to investigate the development of a certain mineral assemblage and investigate the nature of partial melting reactions. Combining experimental studies on partial melting with the geometrical analysis of phase relationships (e.g. Grant, 1985; Vielzeuf and Holloway, 1988) provided at least a reasonable understanding of the underlying melting relationships in rocks. However, fully quantitative thermodynamic calculations on melting using large, internally consistent datasets and complex activity models have evolved mostly over the last fifteen years as more sophisticated activity models for both minerals and melt have been developed (see Holland and Powell, 1998, 2001; White et al., 2001, 2007; White et al., 2011). Experimental studies combined with thermodynamic modelling have now greatly advanced our understanding of partial melting in the upper and lower crust and and this approach provides a comprehensive framework for the interpretation of migmatites, residual granulites and granites (see White et al., 2011). Experimental investigations of granulite-facies migmatites are therefore particularly important for understanding the origin of high-temperature, H_2O-undersaturated granitic magmas. On the other hand direct comparison to natural high-grade rocks is hampered by the fact that they represent the end-product of a number of metamorphic and deformation processes that operate subsequently after the peak of metamorphism in the deep continental crust.

So far to date only relatively few studies have attempted to model the results of experiments on synthetic or natural compositions (e.g. Johnson et al., 2008; Tajcmanová et al., 2009;

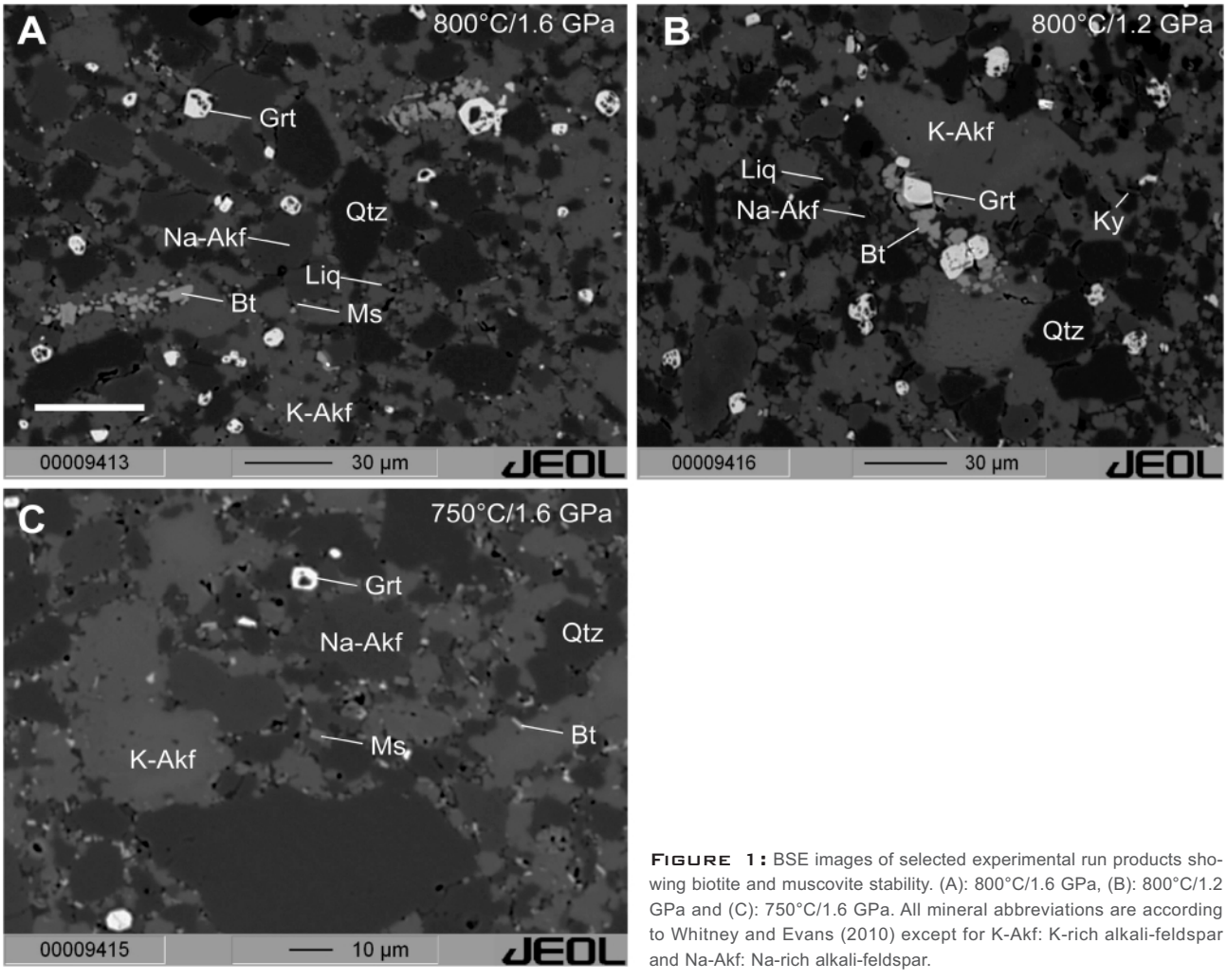

Figure 1: BSE images of selected experimental run products showing biotite and muscovite stability. (A): 800°C/1.6 GPa, (B): 800°C/1.2 GPa and (C): 750°C/1.6 GPa. All mineral abbreviations are according to Whitney and Evans (2010) except for K-Akf: K-rich alkali-feldspar and Na-Akf: Na-rich alkali-feldspar.

Grant, 2009; White et al., 2011). The nature of the chemical system used in the experiment dictates whether experiments and theoretical calculations can directly be compared or not. For instance a direct comparison of thermodynamic modelling and experiments can be undertaken if the experimental composition used is in the same system as the composition used in the modelling (e.g. KFMASH or NCKFMASH). Unfortunately a greater challenge arises when the composition used in the experiments is a natural rock powder that contains many components not accounted for in thermodynamic modelling (e.g. Mn, Ti, Fe^{3+}, Cr, Zn, F, Cl etc.). Here, direct constraints which of a large number of potential sources is responsible for differences in the results is extremely difficult (White et al., 2011). Nevertheless, these experiments still do provide useful constraints on the metamorphic evolution (*P-T-X*) of high-grade rocks and when combined with thermodynamic calculations activity/composition relationships of minerals can be tested. While calculations can be undertaken in increasingly large chemical systems today such as NCKFMASHTO (Na_2O-CaO-K_2O-FeO-MgO-Al_2O_3-SiO_2-H_2O-TiO_2-Fe_2O_3) such systems represent still a significant simplification of nature and the effects of other components on the phase equilibria are still unconstrained.

1.2 High-*P*/high-*T* granulites in the Bohemain Massif

Felsic granulites with the assemblage quartz + ternary feldspar (mesoperthite) + garnet + rutile ± kyanite are a prominent lithology of the Moldanubian domain (Schulmann et al., 2005, 2008; Guy et al., 2010; Lexa et al., 2011). The protolith rock was most likely an effectively dry granite (e.g. Kotková and Harley, 1999; Finger et al., 2003; Janoušek et al., 2004, 2006; Tropper et al., 2005; Janoušek and Holub, 2007) with a low modal abundance of biotite and the absence of visible melt segregations implying that these rocks were fluid-deficient during metamorphism. This view is supported by the low modal proportion of melt (<3 vol.%.) calculated in *P-T* pseudosections by Tajcmanová et al. (2006, 2009, 2010), Štípská et al. (2010) and Franek et al. (2011). This feature is not supported by the experimental investigations of Tropper et al. (2005) who concluded that both, the high-P, high-T formation stage and the subsequent exhumation to mid crustal levels, took place in the presence of a partial melt. Tropper et al. (2005) tried to assess the processes of high-P/high-T granulite formation by conducting fluid-absent piston cylinder experiments using a granitic gneiss with the assemblage K-feldspar + plagioclase + quartz + biotite + muscovite as starting material. The experimental conditions were chosen to simulate the metamorphic *P-T* path determined for the granulites, with runs at 750-1000 °C/1.6 GPa, (prograde path) and 950 °C/1.4 GPa and 800-900 °C/1.2 GPa (retrograde path). The results of their study were consistent with the model of Roberts and Finger (1997) for granulite formation in the South Bohemian Massif,

Run #	P (GPa)	T (°C)	Observed assemblages	THERIAK-DOMINO
JKI-39	1.6	750	Grt + Bt + Na-Akf + K-Akf + Ms + Ky + Rt	Grt + Bt + Na-Akf + K-Akf + Ms + Liq + Ilm
JKI-38	1.6	800	Grt + Bt + Na-Akf + K-Akf + Ms + Ky + Liq + Rt	Grt + Na-Akf + K-Akf + Ms + Liq + Ilm
JKI-35	1.6	850	Grt + Na-Akf + K-Akf + Ky + Liq + Rt	Grt + Na-Akf + K-Akf + Ky + Liq + Rt + Ilm
JKI-24	1.6	900	Grt + K-Akf + Ky + Liq	Grt + K-Akf + Na-Akf + Ky + Liq + Rt
JKI-21	1.6	1000	Grt + K-Akf + Ky + Liq	Grt + K-Akf + Ky + Liq + Rt
JKI-31	1.4	950	Grt + Pl + K-Akf + Ky + Liq + Rt	Grt + Na-Akf + K-Akf + Ky + Liq + Ilm
JKI-36	1.2	800	Grt + Bt + Pl + K-Akf + Ky + Liq + Rt	Grt + Na-Akf + K-Akf + Ky + Liq + Ilm
JKI-33	1.2	900	Grt + K-Akf + Sill + Liq + Rt	Grt + K-Akf + Na-Akf + Sill + Liq + Ilm

Run #	P (GPa)	T (°C)	PERPLEX
JKI-39	1.6	750	Grt + Na-Akf + K-Akf + Ms + Rt
JKI-38	1.6	800	Grt + Na-Akf + K-Akf + Ms + Liq + Rt
JKI-35	1.6	850	Grt + Na-Akf + K-Akf + Ky + Liq + Rt
JKI-24	1.6	900	Grt + K-Akf + Ky + Liq + Rt
JKI-21	1.6	1000	Grt + K-Akf + Ky + Liq + Rt
JKI-31	1.4	950	Grt + K-Akf + Ky + Liq + Rt
JKI-36	1.2	800	Grt + Na-Akf + K-Akf + Ky + Liq + Rt
JKI-33	1.2	900	Grt + K-Akf + Sill + Liq + Rt

Quarz is in excess. All mineral abbreviations are according to Whitney and Evans (2010) except for K-Akf: K-rich alkali-feldspar and Na-Akf: Na-rich alkali-feldspar. Calculated phases with with an abundance of <0.01 moles are omitted from the Table.

Table 1: Piston-cylinder experiment conditions, observed and calculated mineral assemblages using THERIAK-DOMINO and PERPLEX.

according to which both, the high-*P*, high-*T* formation stage and the subsequent exhumation to mid crustal levels, took place in the presence of a partial melt. However they also noted that the modal amounts of melt observed in the experiments were generally much higher than those modelled by Roberts and Finger (1997).

Due to the anhydrous, high-*T* high-*P* nature of the experiments and the relatively simple phase assemblage obtained (e.g. no amphiboles) the experimental investigation of Tropper et al. (2005) in the metagranitic system represents an ideal case for a comparison between thermodynamic calculations and experimental results which was the impetus for this study.

2. Petrography of the experiments by Tropper et al. (2005)

Tropper et al. (2005) conducted experiments at 750°C/1.6 GPa, 800°C/1.6 GPa, 850°C/1.6 GPa, 900°C/1.6 GP and 1000°C/1.6 GPa (prograde path) and 950°C/1.4 GPa, 900°C/1.2 GPa and 800°C/1.2 GPa (retrograde path). The experiments in the temperature range 850-1000°C all yielded the typical granulite assemblage garnet + K-rich alkali-feldspar (Ab28-48) ± Na-rich alkali-feldspar (Ab_{63-92}) + quartz ± kyanite ± rutile (Table 1). At 1000°C/1.6 GPa roughly 30 to 40 vol.% partial melt was present, and large melt volumes persisted also on the retrograde path (>40! vol.% at 950°C/1.4 GPa, ~25 vol.% at 900°C/1.2 GPa, Table 1). The high-P (>1.6 GPa) melt-forming reaction observed in the experiments is (Grant, 1985; Vielzeuf and Holloway, 1988; Vielzeuf and Schmidt, 2001):
Biotite + Plagioclase + Muscovite + Quartz = Garnet + ternary Alkali-feldspar + Melt

At pressures of 1.6 GPa, this reaction commences at temperatures >750°C and goes to completion between 800°C and 850°C. In the isobaric section at 1.6 GPa, both biotite and muscovite are present at 750°C and 800°C. Up to 850°C, two feldspars (K-rich- and Na-rich alkali-feldspar) are present in the experiments. In runs at 900°C and 1000 °C the assemblage garnet + K-rich alkali-feldspar + kyanite + melt is stable. Experiments at 1.2 GPa show assemblages and textures similar to runs at 1.6 GPa with biotite being stable up to 800°C and Na-rich alkali-feldspar disappears between 800°C and 900°C. Muscovite was not observed in the 1.2 GPa runs. Selected observed phase relations concerning biotite and muscovite stability are shown in Figure 1.

Tropper et al. (2005) infered that equilibrium was approached reasonably well based on systematic changes in phase compositions and proportions with *T* (and *P*). As an additional test they calculated pressures using the GASP barometer reaction 3anorthite = grossular + 2kyanite + quartz and resulting pressures were in good agreement with nominal run pressures and reproduced the experimental *P*-conditions to within 0.15-0.2 GPa. In this study we applied the two-feldspar geothermometer to test whether temperatures could also be reproduced in runs where two feldspars were present. To account for possible compositional modification of feldspar compositions equilibration temperatures were calculated with an EXCEL spreadsheet using the two-feldspar thermometer expression of Benisek et al. (2004) and the feldspar mixing model of Benisek et al. (2010). The rationale for using the Benisek et al. (2004) method is their consideration of resetting of feldspar compositions according to the approach of Kroll et al. (1993), which corrects for compositional modifications due largely different diffusion kinetics which occur between the coupled substitution $CaAlNa_{-1}Si_{-1}$ and the simple ionic substitutions NaK_{-1} by minimizing the variance in the calculated temperatures by changing feldspar compositions along the albite-K-feldspar join. By using the compositional data of the feldspars from Tropper et al. (2005, Tables 6A, B) the resulting temperatures are 794°C for the 750°C/1.6 GPa experiment (JKI-39), 798°C for the 800°C/1.6 GPa experiment (JKI-38), 838°C for the 850°C/1.6 GPa experiment (JKI-35) and 754°C for the 800°C/1.2 GPa experiment (JKI-36). The deviations in two experiments (750°C/1.6 GPa and 800°C/1.2 GPa) indicates most likely a lack of equilibration in these experiments, which can be tested by using the pseudosection technique.

3. Analytical methods

Electron microprobe analysis: A JEOL 8100 SUPERPROBE electron microprobe was used for analysing biotite and muscovite compositions at the Institute of Mineralogy and Petrography at the University of Innsbruck. Analytical conditions were 15 kV acceleration voltage and 10 nA beam current. Natural and synthetic mineral standards were used for calibration. The counting times were 20 sec. for the peak and 10 sec. for the background.

Pseudosection calculations: The bulk composition for the pseudosection calculations in the system KNCFMMnTiASH from Tropper et al. (2005) is: SiO_2: 77.40%; Al_2O_3: 12.30%; CaO: 0.54%; K_2O: 4.64%; Na_2O: 2.87%; MnO: 0.02 %, MgO: 0.18%; FeO: 1.69%; H_2O: 0.40%.

THERIAK-DOMINO (De Capitani and Petrakakis, 2010): Pseudosection calculations were undertaken using the updated version of the internally consistent data set of Holland and Powell (1998, data set tcdb55c2d), and extended *A-X* models after White et al. (2001, 2007).

PERPLEX (Connolly and Petrini, 2005): The activity models used in the calculations are: garnet and melt after White et al. (2001, 2007); biotite after Tajcmanova et al. (2009), feldspar after Benisek et al. (2010) and muscovite after Chatterjee and Froese (1975) extended with an ideal phengite solution model. In order to test different models for biotite and muscovite the activity model of White et al. (2007) for biotite and the model of Coggon and Holland (2002) with extensions from Auzanneau et al. (2010) for muscovite were also used for comparison.

4. Results

4.1 Comparison between observed and calculated mineral assemblages using THERIAK-DOMINO

Figure 2A shows the pseudosection in the system KNCF-

MMnTiASH calculated with THERIAK-DOMINO and Table 1A gives the calculated mineral assemblages for each experiment and Table 2A gives the observed and calculated mineral modes. In the experiments at 1.6 GPa biotite is stable in the 750°C and 800°C experiments, while in the calculations biotite occurs only at 750°C at 1.6 GPa. Muscovite is stable in the 750°C and 800°C experiments at 1.6 GPa, which also agrees with the calculations since the calculated muscovite stability field terminates between 850°C and 900°C at 1.6 GPa. Na-rich alkali-feldspar is stable in the 850°C experiment while the calculations predict a larger stability field up to 950°C (Fig. 2A). Although in the 750°C and 1.6 GPa experiment, no melting was visible (perhaps due to the very low degree of melting) the calculations predict melting to begin slightly below 750°C at 1.6 GPa as can be seen in Figure 2A. In the 1.2 GPa experiments at 800°C and 900°C neither biotite nor muscovite should occur according to the calculations but biotite does occur at 800°C. Na-rich alkali-feldspar also occurs at 900°C and 1.2 GPa according to the calculations (Fig. 2A). In contrast to the observed mineral assemblages the calculations yielded ilmenite (<0.1 moles) in some of the experiments. Table 2A shows the comparison between the observed and calculated modal proportions of the minerals and Figue 3A shows the modal evolution of K-rich alkali-feldspar, Na-rich alkalifeldspar and melt as a function of T at 1.6 GPa. Figure 3A shows that the observed and calculated modal trends concerning K-rich alkali-feldspar strongly differ. While the observed modal amounts indicate decreasing K-rich alkali-feldspar contents, the calculations yield increasing contents. Although the modal trends for Na-rich alkali-feldspar and melt agree with their directions, the absolute amounts strongly differ. While in the experiments more than 30 vol.% melt were observed the calculations only yielded up to 10 vol.%! also the calculations predict lower Na-rich alkali-feldspar contents (7 vol.%) than the actual observations (18 vol.%) at 750°C.

4.2 Comparison between observed and calculated mineral assemblages using PERPLEX

Figure 2B shows the pseudosection in the system KNCF-MMnTiASH calculated with PERPLEX and Table 1 again gives

Run#:	JKI-39	JKI-38	JKI-35	JKI-24	JKI-21	JKI-31	JKI-36	JKI-33
P-T	750/1.6	800/1.6	850/1.6	900/1.6	1000/1.6	950/1.4	800/1.2	900/1.2
	obs/calc	obs/calc	obs/calc	obs/calc	obs/calc	obs/calc	obs/calc	obs/calc
K-Akf	37/30	56/34	44/41	42/44	33/49	26/49	44/39	47/45
Grt	3/3	2/3	2/3	2/3	<1/2	1/2	2/3	2/3
Qtz	37/41	30/40	38/39	25/39	33/38	32/39	45/39	27/39
Melt	0/1	3/2	16/5	31/6	33/10	41/9	3/5	23/8
Na-Akf	18/19	7/16	<1/11	0/7	0/0	0/1	6/13	0/5
Other	5/7	2/5	0/1	0/1	0/1	0/1	0/1	<1/1

Obs: observed; calc: calculated; due o their small modal occurrence, the amounts of biotite,kyanite, rutile and muscovite could not be distinguished separately and are combined as other phases. **A**

Run#:	JKI-39	JKI-38	JKI-35	JKI-24	JKI-21	JKI-31	JKI-36	JKI-33
P-T	750/1.6	800/1.6	850/1.6	900/1.6	1000/1.6	950/1.4	800/1.2	900/1.2
	obs/calc	obs/calc	obs/calc	obs/calc	obs/calc	obs/calc	obs/calc	obs/calc
K-Akf	37/21	56/23	44/34	42/51	33/49	26/50	44/37	47/50
Grt	3/3	2/3	2/3	2/3	<1/3	1/3	2/3	2/3
Qtz	37/41	30/40	38/39	25/39	33/38	32/38	45/39	27/38
Melt	0/0	3/1	16/5	31/6	33/9	41/8	3/5	23/8
Na-Akf	18/27	7/27	<1/18	0/0	0/0	0/0	6/15	0/0
Other	5/8	2/6	0/1	0/1	0/1	0/1	0/1	<1/1

Obs: observed; calc: calculated; due to their small modal occurrence, th amounts of biotite, kyanite, rutile and muscovite could not be distinguished separately and are combined as other phases. **B**

Table 2: A: Observed and calculated modal proportions (vol.%) of the run products using THERIAK-DOMINO. B: Observed and calculated modal proportions (vol.%) of the run products using PERPLEX.

the calculated mineral assemblages and Table 2B gives the observed and calculated mineral modes for each experiment. In the calculations biotite is not stable at the P-T conditions where experiments were conducted but muscovite occurs at the same conditions as in the experiments at 750°C and 800°C at 1.6 GPa. Na-rich alkali-feldspar is also stable only up to 850°C experiment and the calculated onset of melting occurs slightly below 800°C. Again in the 1.2 GPa experiments at 800°C and 900°C neither biotite nor muscovite occur according to the calculations and Na-rich alkali-feldspar also occurs only up to 850°C and 1.2 GPa. Similar to the observations the calculations yielded only rutile (0.1 vol.%) and no ilmenite. Figue 3B shows the modal evolution of K-rich alkali-feldspar, Na-rich alkali-feldspar and melt as a function of T at 1.6 GPa. Similar to Figure 3A the observed and calculated modal trends concerning K-rich alkali-feldspar strongly differ. While the observed modal amounts indicate decreasing K-rich alkali-feldspar contents, the calculations yield strongly increasing contents especially >900°C. Although the directions of the modal trends for Na-rich alkali-feldspar and melt agree, the absolute amounts differ strongly for both. While in the experiments less than 10 vol.% Na-rich alkali-feldspar occur, the calculations yielded more than 25 vol.% below 800°C! The calculated amount of melt is also very low (<10 vol.%) when compared with the experiments (>30 vol.%).

Table 1 shows that both programs show a similar level of success in the comparison between predicted thermodynamically stable mineral assemblages and observed assemblages, but one has to keep in mind that in both calculations different activity models were used. So a direct comparison between both programs is indeed not possible and hence we only highlight certain features from both calculations to illustrate to comparison between the experimental and computational results. While the agreement between the observed and calculated mineral assemblages (Na-rich alkaki-feldspar stability at 1.6 GPa, onset of melting, presence of rutile) is slightly better when using PERPLEX with the selected activity models, THERIAK-DOMINO predicts biotite to be stable at least at 750°C/1.6 GPa and also predicts Na-rich alkali-feldspar to be stable at 950°C/1.4 GPa (Table 1). On the other hand when looking at the absolute modal amounts large deviations occur in both calculations (Figs. 3A, B). Both calculations predict similar amounts of melt (<10 vol.%) which are in strong contrast to the experimental results. It is also noteworthy that both calculations yieded a discrepancy between observed and calculated biotite stability regions (Table 1). In the calculations using THERIAK-DOMINO biotite at least occurs at 750°C/1.6 GPa while in the calculations using PERPLEX biotite is not stable at any of the experimental conditions. On the other hand muscovite stability was correctly calculated at 750°C and 800°C at 1.6 GPa using both programs and the activity models (Table 1). One of the reasons for the discrepancy concerning biotite stability could be the occurrence of minor element substitution in biotite not accounted for in the experimental investigations of Tropper et al. (2005). Sample Fi12/94 which was used for the experiments contained ca. 1000 ppm F. Hence significant F substitution in biotite and muscovite could occur which was not investigated by Tropper et al. (2005). Therefore in the course of this study a wavelength-dispersive (WDS) re-investigation of mica com-

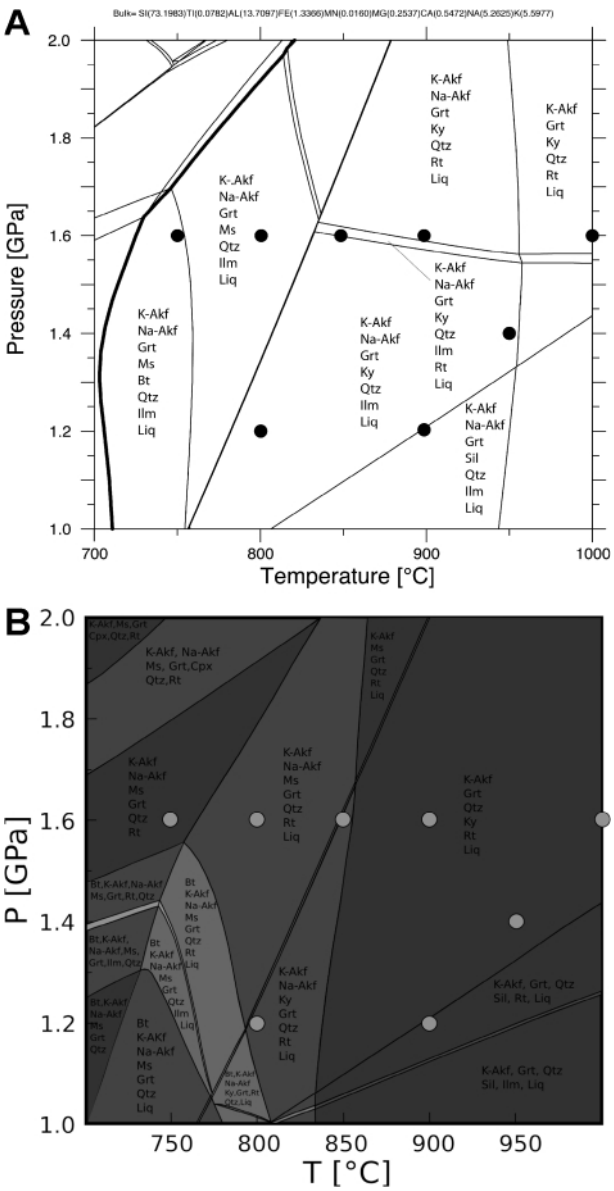

Figure 2: A: THERIAK-DOMINO pseudosection of starting material Fi94 in the system K_2O-Na_2O-CaO-MnO-FeO-MgO-Al_2O_3-TiO_2-SiO_2-H_2O (KNCMnFMATSOH) and using the *a-X* relations from White et al. (2001, 2007). The relevant mineral assemblages and their stability fields are shown. Black circles indicate the *P-T* conditions of the experiments from Tropper et al. (2005). Calculated phases with abundances <0.01 vol.% have been omitted from the diagram. The thick line indicates the onset of melting. B: PERPLEX pseudosection of starting material Fi94 in the system K_2O-Na_2O-CaO-MnO-FeO-MgO-Al_2O_3-TiO_2-SiO_2-H_2O (KNCMnFMATSOH) using the *a-X* relations of garnet and melt after White et al. (2001, 2007); biotite after Tajcmanova et al. (2009), feldspar after Benisek et al. (2010) and muscovite after Chatterjee and Froese (1975). The relevant mineral assemblages and their stability fields are shown. Black circles indicate the *P-T* conditions of the experiments. Calculated phases with abundances <0.01 vol.% have also been omitted from the diagram. All mineral abbreviations are according to Whitney and Evans (2010) except for L: melt.

positions with special emphasis on F and Cl was undertaken.

5. Mineral chemistry

5.1 Biotite and muscovite analyses from the experiments of Tropper et al. (2005)

Mineral formulae of biotite and muscovite were calculated on a basis of 11 oxygens. Chemical analyses of both minerals are given in Table 3. For comparison additional mica analyses (although without F and Cl) are in Tropper et al. (2005, Table 7).

Biotite: Biotite is stable in three experiments at 750°C/1.6 GPa, 800°C/1.6 GPa and 800°C/1.2 GPa. In contrast to the EDS analyses from Tropper et al. (2005) biotite contains significant F contents ranging from 1.68 ± 0.19 wt.% to 2.51 ± 0.11 wt.%. This corresponds to F contents of 0.411 ± 0.048 to 0.584 ± 0.027 a.p.f.u. F also shows a positive correlation with increasing *T* from 750°C to 800°C at 1.6 GPa. The Cl contents are low at all conditions with 0.12 ± 0.02 wt.%.

Muscovite: Muscovite was observed only in two experiments at 750°C/1.6 GPa and 800°C/1.6 GPa coexisting with biotite. Again in contrast to the EDS analyses given by Tropper et al. (2005) significant F contents of 1.46 ± 0.05 wt.% and 1.88 ± 0.09 wt.% occur. This corresponds to increasing F contents of 0.305 ± 0.011 (750°C/1.6 GPa) and 0.392 ± 0.018 a.p.f.u. (800°C/1.6 GPa). The Cl contents are very low at all conditions with up to 0.03 ± 0.03 wt.%.

5.2 Observed and calculated mineral compositions using THERIAK-DOMINO and PERPLEX

Figures 4A-F and Tables 4A, B show the comparison between the observed and calculated mineral compositions of garnet, K-rich alkali-feldspar and Na-rich alkali-feldspar as a function of T at 1.6 GPa using THERIAK-DOMINO (Figs. 4A, C, E) and PERPLEX (Figs. 4B, D, F). The observed compositions of garnet and feldspars are from Tropper et al. (2005, Tables 5, 6A, B).

THERIAK-DOMINO: While the amount and trend of the grossular component agrees between calculations and observations, pyrope contents differ but the trend is predicted correctly (Fig. 4A). In contrast almandine contents differ with respect to the amount and the trend evolution since the observation yielded decreasing almandine content and the calculations yielded increasing almandine contents (Fig. 4A). On the other hand, the agreement between observed and calculated components of K-rich alkali-feldspar is very good (Fig. 4C). The agreement between observed and calculated components and their compositional trends in coexisting Na-rich alkali-feldspar is very good only up to 800°C, at 850°C the observed albite component is much lower while the observed K-feldspar component is much higher (Fig. 4E). The Ti content of biotite of 0.11 a.p.f.u. at 750°C and 1.6 GPa agrees very well with the calculations (0.11 a.p.f.u.) also Si contents of muscovite of 3.30 a.p.f.u. at 750°C and 3.19 a.p.f.u.at could be reproduced satisfactorily (Table 4A).

PERPLEX: Figure 4B shows a very similar compositional evolution of garnet to the calculations using THERIAK-DOMINO (Fig. 4A) only the predicted grossular contents are slightly lower when using PERPLEX. The agreement between observed and calculated components of K-rich alkali-feldspar is also very good (Fig. 4D). The agreement between observed and calculated components and their compositional trends in coexisting Na-rich alkali-feldspar is not good since the calculated albite component is significantly lower while the K-feldspar

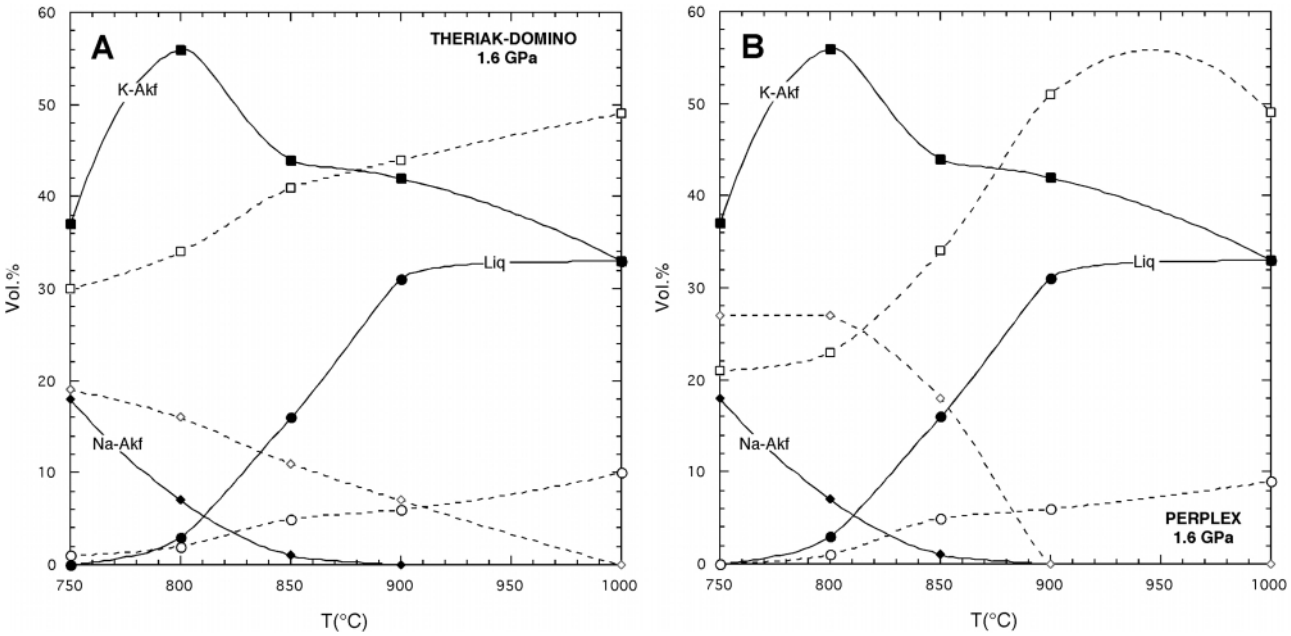

Figure 3: Calculated (open symbols) vs. observed (black symbols) modal amounts of K-rich alkali-feldspar (K-Akf, square), Na-rich alkalifeldspar (Na-Akf, diamond) and melt (Liq, circle) as a function of *T* at 1.6 GPa with (A) THERIAK-DOMINO and (B) PERPLEX. The continuous and dashed lines show the observed and calculated trends.

Run#:	JKI 39		JKI 38		JKI 36		JKI 39		JKI 38	
P-T	750/1.6		800/1.6		800/1.2		750/1.6		800/1.6	
n:	8	1σ	7	1σ	6	1σ	6	1σ	6	1σ
Phase	Bt		Bt		Bt		Ms		Ms	
SiO_2	37.46	1.27	40.49	1.31	38.31	1.77	50.86	1.36	49.70	1.18
TiO_2	1.97	0.20	4.11	0.64	4.33	0.32	0.34	0.06	0.74	0.17
Al_2O_3	19.51	0.28	19.52	0.46	19.95	0.26	28.36	1.22	30.05	0.99
Cr_2O_3	0.01	0.02	0.01	0.01	0.01	0.01	0.01	0.01	0.01	0.01
FeO	23.02	1.17	16.25	0.40	14.78	0.84	5.52	0.78	3.66	0.35
MnO	0.10	0.04	0.08	0.02	0.12	0.05	0.03	0.03	0.01	0.01
MgO	2.95	0.15	5.57	0.32	8.31	0.15	1.09	0.08	1.85	0.10
CaO	n.d.	n.d.	n.d.	n.d.	0.01	0.02	0.09	0.10	0.01	0.03
Na_2O	0.31	0.11	0.58	0.13	0.39	0.16	0.99	0.19	0.89	0.24
K_2O	9.30	0.32	9.15	0.23	9.45	0.41	9.84	0.26	9.89	0.26
F	1.68	0.19	2.16	0.14	2.51	0.11	1.46	0.05	1.88	0.09
Cl	0.12	0.02	0.12	0.01	0.12	0.02	0.01	0.01	0.03	0.03
H_2O^a	3.06	0.12	3.04	0.11	2.86	0.08	3.84	0.05	3.65	0.05
-Cl,F=O	0.71	0.08	0.91	0.06	1.06	0.05	0.61	0.02	0.79	0.04
Σ	98.79	0.63	100.17	1.16	100.09	0.68	101.82	0.36	101.59	0.47
Si	2.889	0.065	2.964	2.964	2.811	0.085	3.366	0.076	3.276	0.061
Al(IV)	1.111	0.065	1.036	1.036	1.189	0.085	0.634	0.076	0.724	0.061
Sum T	4.000	-	4.000	-	4.000	-	4.000	-	4.000	-
Al(VI)	0.663	0.052	0.648	0.040	0.536	0.061	1.578	0.044	1.610	0.027
Ti	0.114	0.011	0.226	0.034	0.239	0.021	0.017	0.003	0.037	0.008
Cr	0.012	<0.001	0.012	<0.001	0.012	<0.001	0.010	0.000	0.010	0.000
Fe^{2+}	1.486	0.094	0.995	0.032	0.908	0.065	0.306	0.044	0.202	0.020
Mn	0.007	0.003	0.005	0.001	0.007	0.003	0.002	0.002	0.001	0.001
Mg	0.340	0.018	0.608	0.041	0.909	0.018	0.107	0.009	0.181	0.010
Vac.	0.377	0.053	0.506	0.044	0.389	0.039	-	-	-	-
Σ M(1,2)	3.000	-	3.000	-	3.000	-	2.020	0.029	2.041	0.033
Ca	n.d.	n.d.	n.d.	n.d.	0.001	0.001	0.006	0.007	0.001	0.002
Na	0.047	0.017	0.082	0.082	0.055	0.055	0.128	0.025	0.114	0.031
K	0.915	0.036	0.855	0.855	0.885	0.885	0.830	0.026	0.832	0.027
Vac.	0.038	0.024	0.063	0.063	0.059	0.059	-	-	-	-
Σ A	1.000	-	1.000	-	1.000	-	0.964	0.032	0.947	0.040
F	0.411	0.048	0.500	0.037	0.584	0.027	0.305	0.011	0.392	0.018
Cl	0.016	0.003	0.015	0.015	0.015	0.015	0.001	0.001	0.004	0.005
OH	1.573	0.049	1.485	0.036	1.401	0.026	1.693	0.012	1.604	0.015
Σ	2.000	-	2.000	-	2.000	-	2.000	-	2.000	

n.d.: not detected; biotite and muscovite calculated on the basis of 11 oxygens; n: number of analyses; [a]H_2O:calculated.

Table 3: Biotite and muscovite analyses from the experiments.

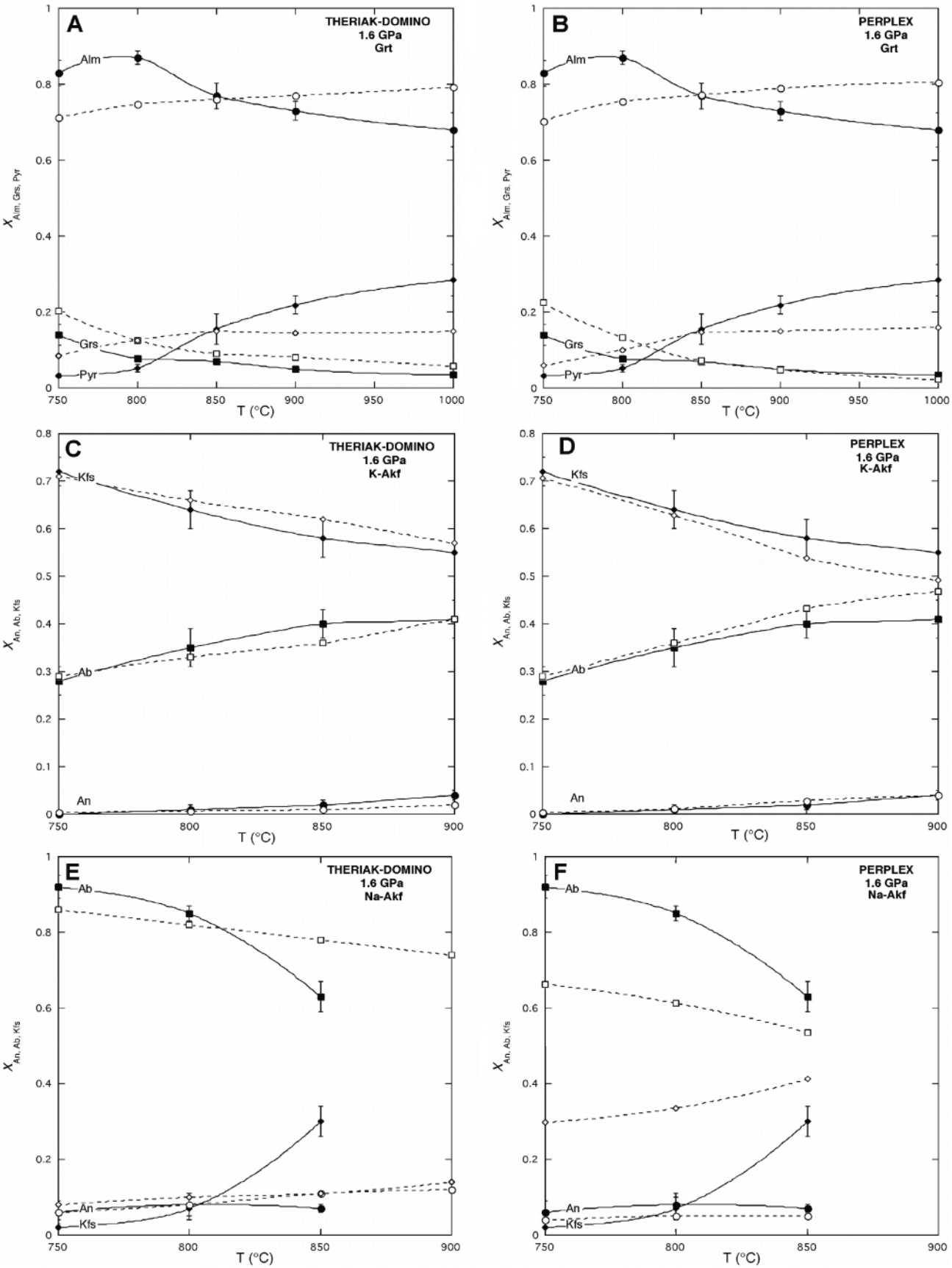

Figure 4: Calculated (open symbols) vs. observed (black symbols) mineral compositions of garnet (A, B), K-rich alkali-feldspar (C, D) and Na-rich alkali-feldspar (E, F) as a function of *T* at 1.6 GPa with THERIAK-DOMINO (A, C, E) and PERPLEX (B, D, F). Calculated (open symbols) vs. observed (black symbols) mineral compositions of garnet (D), K-rich alkali-feldspar (E) and Na-rich alkali-feldspar (F) as a function of *T* at 1.6 GPa with PERPLEX. The variables in (A, B) are: almandine (circles), pyrope (squares) and grossular (diamonds). The variables in (C, D) are: K-feldspar (circles), albite (squares) and anorthite (diamonds) and the variables in (E, F) are: albite (circles), anorthite (squares) and K-feldspar (diamonds). The observed mineral compositions are from Tropper et al. (2005, Tables 5, 6A, B).

component is higher compared to the experiments (Fig. 4F). No Ti contents of biotites could be calculated and the Si contents of muscovites of 3.42 a.p.f.u. at 750°C and 3.32 a.p.f.u. are slightly higher than observed in experiments (Table 4B).

6. Discussion

Comparison between observed and calculated biotite stability: Despite using different activity models both calculations of this study show an underestimation of biotite stability with respect to the experimental observations from Tropper et al. (2005). While THERIAK-DOMINO with activity models from White et al. (2001, 2007) correctly predict biotite stability at 750°C/1.6 GPa, which still underestimates the observed stability by <100°C, no stable biotite could be calculated using PERPLEX even when the most recent biotite activity model of Tajcmanová et al. (2009) is used. This discrepancy between calculated and observed biotite stability has already been observed by Tajcmanová et al. (2009) who made a comparison of biotite compositions predicted with the White et al. (2007) solution model and experimental determinations (Vielzeuf and Montel, 1994) for a metagreywacke composition. This revealed that at granulite-facies conditions the predicted Ti-content of biotite was significantly lower than the experimentally observed Ti content. The stability of biotite is not only a function of additional elemental substitutions but also a function of the other activity models used in the calculations and hence can vary strongly depending on the models used for white mica, feldspars etc. In order to explore the influence of a different muscovite activity model on biotite stability two pseudosections were calculated (Fig. 6A, B). The first pseudosection uses the muscovite activity model of Coggon and Holland (2002) and the extension of Azanneau et al. (2010) and the biotite activity model of White et al. (2007) as shown in Figure 6A. The second calculation uses the same muscovite activity model but the more recent biotite activity model of Tajcmanova et al. (2009) and is shown in Figure 6B. The biotite stability field in both calculations (Figure 6A,B) is even smaller when compared to the stability predicted using the Chatterjee and Froese (1975) muscovite model with ideal phengite extension (Figure 2B). Thus the discrepancy in biotite stability between the THERIAK-DOMINO and PERPLEX calculations is mainly due to the use of different feldspar models, which is from Baldwin et al. (2005) based on the model of Holland and Powell (2003) in THERIAK-DOMINO and from Benisek et al. (2010) in PERPLEX. Since the Chatterjee and Froese (1975) model does not account for Ti, rutile is stable in biotite-absent phase fields since no other mineral solution model incorporates Ti. Nevertheless the Chatterjee and Froese (1975) muscovite model with the ideal phengite extension has been shown in our study to better reproduce the observed Si contents of muscovites than any other muscovite model so far.

The role F in biotite and muscovite: The presence of F and Ti in natural biotite has significanct effects on the temperature of fluid-absent melting reactions associated with granulite-facies metamorphism of crustal rocks. The increase in the thermal stability of F-bearing over OH mica was reported by Munoz and Luddington (1974), Peterson et al. (1991) and Valley et al. (1992), and a similar effect for Ti-bearing micas has been reported by Tronnes et al. (1985) and Patiño Douce (1993). The combined effect of the F and Ti content in phlogopite on ist stability temperatures in the KMASH system has been found to be additive in relation to those containing only F or Ti. The behavior of phlogopite in the F-bearing system was experimentally studied by Peterson et al. (1991), who determined the fluid-absent melting relations of the assemblage F-rich phlogopite + quartz. Dooley and Patiño-Douce (1996) investigated

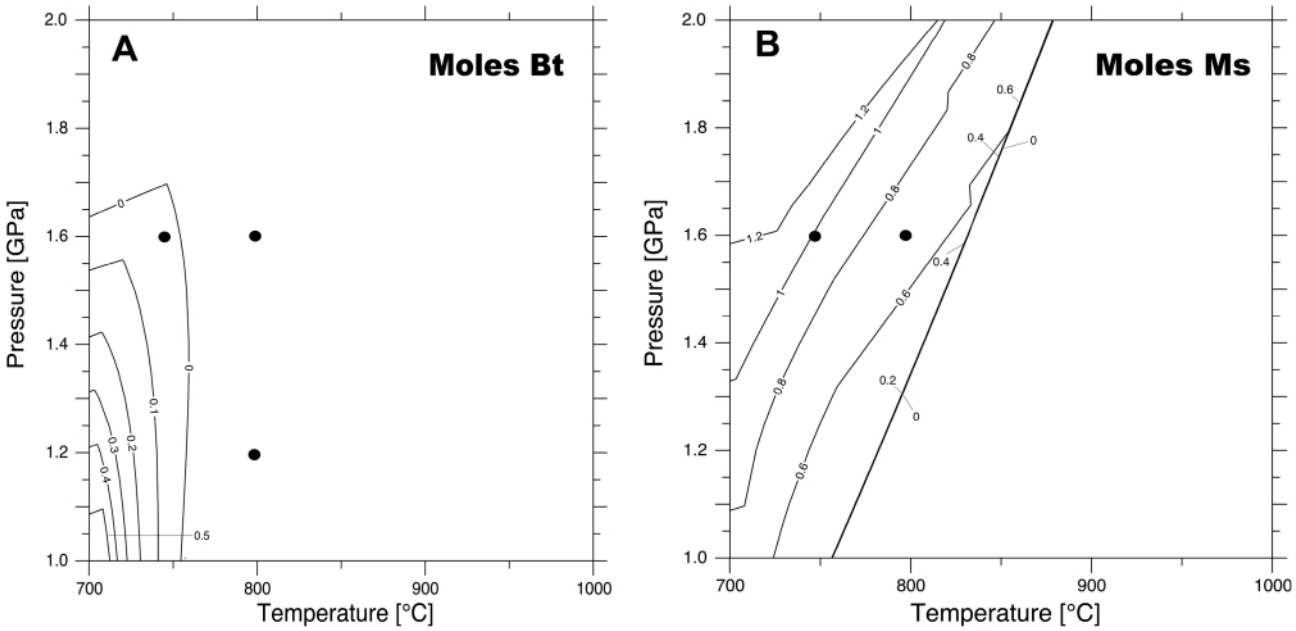

Figure 5: Calculated stability fields of biotite (A) and muscovite (B) using THERIAK-DOMINO and the *a-X* expressions from White et al. (2001, 2007). The black circles indicate the *P-T* conditions where biotite and muscovite are stable in the experiments of Tropper et al. (2005).

the reaction F-phlogopite + quartz + rutile = enstatite + melt. Their results indicate that the thermal stability of F-rich phlogopite + quartz + rutile is extended by as much as 450°C relative to the KMASH system and by 300°C relative to the Ti-free KFMASH system. The most recent biotite activity models are from White et al. (2007) and Tajcmanova et al. (2009) which consider Fe^{3+} and Ti in the system KFMASHTO by introducing titanium biotite and ferric biotite end-members. The difference between both models lies in the fact that Tajcmanova et al. (2009) assume Ti to mix on the M2 site while White et al. (2007) assume it to mix on the M1 site. While both models consider O substitution on the OH site, equivavlent to

Run#:	JKI-39	JKI-38	JKI-35	JKI-24	JKI-21	JKI-31	JKI-36	JKI-33
P-T	750/1.6	800/1.6	850/1.6	900/1.6	1000/1.6	950/1.4	800/1.2	900/1.2
	obs/calc	obs/calc	obs/calc	obs/calc	obs/calc	obs/calc	obs/calc	obs/calc
X_{Alm}	0.83/0.71	0.87/0.75	0.77/0.76	0.73/0.77	0.68/0.79	0.74/0.79	0.87/0.80	0.78/0.80
X_{Grs}	0.13/0.20	0.08/0.13	0.07/0.09	0.05/0.08	0.03/0.06	0.21/0.05	0.05/0.04	0.04/0.04
X_{Pyr}	0.03/0.09	0.05/0.13	0.15/0.15	0.21/0.15	0.28/0.15	0.01/0.16	0.08/0.16	0.18/0.16
$X_{Kfs, K\text{-}Akf}$	0.72/0.70	0.64/0.67	0.58/0.62	0.55/0.57	0.47/0.52	0.60/0.52	0.65/0.65	0.55/0.55
$X_{Ab, K\text{-}Akf}$	0.28/0.29	0.35/0.33	0.40/0.36	0.41/0.41	0.48/0.45	0.38/0.45	0.34/0.34	0.41/0.42
$X_{An, K\text{-}Akf}$	<0.01/<0.01	0.01/0.01	0.02/0.01	0.04/0.02	0.05/0.04	0.02/0.04	0.01/0.01	0.04/0.03
$X_{Kfs, Na\text{-}Akf}$	0.02/0.08	0.07/0.10	0.30/0.11	-/0.14	-	-/0.15	0.11/0.09	-/0.13
$X_{Ab, Na\text{-}Akf}$	0.92/0.86	0.85/0.82	0.63/0.78	-/0.74	-	-/0.69	0.80/0.77	-/0.71
$X_{An, Na\text{-}Akf}$	0.06/0.06	0.08/0.08	0.07/0.11	-/0.12	-	-/0.16	0.09/0.13	-/0.16
$Ti_{Bt, apfu}$	0.11/0.11	0.23/-	-	-	-	-	0.24/-	-
$Si_{Ms, apfu}$	3.37/3.30	3.28/3.19	-	-	-	-	-	-

Obs: observed; calc: calculated **A**

Run#:	JKI-39	JKI-38	JKI-35	JKI-24	JKI-21	JKI-31	JKI-36	JKI-33
P-T	750/1.6	800/1.6	850/1.6	900/1.6	1000/1.6	950/1.4	800/1.2	900/1.2
	obs/calc	obs/calc	obs/calc	obs/calc	obs/calc	obs/calc	obs/calc	obs/calc
X_{Alm}	0.83/0.70	0.87/0.76	0.77/0.77	0.73/0.79	0.68/0.81	0.74/0.81	0.87/0.80	0.78/0.81
X_{Grs}	0.13/0.22	0.08/0.13	0.07/0.07	0.05/0.05	0.03/0.02	0.21/0.02	0.05/0.04	0.04/0.02
X_{Pyr}	0.03/0.06	0.05/0.10	0.15/0.15	0.21/0.15	0.28/0.16	0.01/0.16	0.08/0.15	0.18/0.16
$X_{Kfs, K\text{-}Akf}$	0.72/0.71	0.64/0.63	0.58/0.54	0.55/0.49	0.47/0.49	0.60/0.49	0.65/0.59	0.55/0.49
$X_{Ab, K\text{-}Akf}$	0.28/0.29	0.35/0.36	0.40/0.43	0.41/0.47	0.48/0.47	0.38/0.47	0.34/0.39	0.41/0.47
$X_{An, K\text{-}Akf}$	<0.01/<0.0	0.01/0.01	0.02/0.03	0.04/0.04	0.05/0.04	0.02/0.04	0.01/0.02	0.04/0.05
$X_{Kfs, Na\text{-}Akf}$	0.02/0.30	0.07/0.34	0.30/0.41	-	-	-	0.11/0.27	-
$X_{Ab, Na\text{-}Akf}$	0.92/0.66	0.85/0.61	0.63/0.54	-	-	-	0.80/0.64	-
$X_{An, Na\text{-}Akf}$	0.06/0.04	0.08/0.05	0.07/0.05	-	-	-	0.09/0.09	-
$Ti_{Bt, apfu}$	0.11/-	0.23/-	-	-	-	-	0.24/-	-
$Si_{Ms, apfu}$	3.37/3.42	3.28/3.32	-	-	-	-	-	-

Obs: observed; calc: calculated **B**

Table 4: A: Comparison between selected observed and calculated compositional parameters using THERIAK-DOMINO. B: Comparison between selected observed and calculated compositional parameters using PERPLEX.

the Ti contents, non of the models considers F or Cl substitution on this site. Substitution of F and Cl on the OH site reduces the $(X_{OH,V})^2$ term in the ideal activity model from 0.94 to 0.73 for biotites from the 750°C and 1.6 GPa experiments and leads a significant reduction of the $(X_{OH,V})^2$ term from 0.88 to 0.58 in the 800°C and 1.2 GPa experiments. These activity reductions should lead to even higher thermal stabilites of biotites as predicted by the models so far, which has been shown in the experiments where it occurs up to 800°C and 1.6 GPa. As shown in the experiments, biotite stability terminates somewhere between 800° to 850°C at 1.6 GPa which is about 50-100°C higher than calculated by THERIAK-DOMINO (Fig. 5) With respect to muscovite only few data exist on F substitution in muscovites (Munoz and Luddington, 1977; Monier and Robert, 1986). Monier and Robert (1986) conducted experimental investigations on muscovite stability at 0.2 GPa and found that F (X_F = 0.3) stabilizes muscovite by ca. 50°C. Auzanneau et al. (2012) extend the model of Coggon and Holland (2002) to consider Ti on the MsB octahedral site but again F and Cl contents on the OH site are not accounted for. When considering F on the OH site the $(X_{OH,V})^2$ term reduces to 0.84 (750°C, 1.6GPa) and 0.80 (800, 1.2 GPa). However, calculations using both programs as carried out in this study correctly predict muscovite to be stable at 750°C and 800°C at 1.6 GPa which is in agreement with the experimental observations. Thus the enlargment of muscovite stability due to F substitution for OH may be much smaller and below 50°C (Fig. 5B).

Thermodynamic equilibrium constraints on the experiments: Tropper et al. (2005) assumed that high temperatures, long durations, geobarometric constraints and the reactivity of phases in the experiments were proof for significant equilibration in the experiments. While this might hold true for high-*T* experiments >850°C the modes (K-rich- and Na-rich alkali-feldspar) and compositions (Na-rich alkali-feldspar, garnet) of minerals <850°C indicate a lack of pervasive equilibration throughout the samples. For instance Na-rich alkali-feldspar composition (X_{Ab} = 0.92) at 750°C/1.6 GPa is very similar to the composition of the starting plagioclase (X_{Ab} = 0.93) and hence a mixture between magmatic and metamorphic feldspar compositions can lead to erroneous geothermometric results (e.g. Štípská and Powell, 2005). This fact has also been corraborated by two-feldspar geothermometry which yielded significant deviations in the lowest *T* experiments namely at 750°C/1.6 GPa and 800°C/1.2 GPa.

Contrasting amounts of melt: The results of Tropper et al. (2005) are consistent with the model of Roberts and Finger (1997) for granulite formation in the South Bohemian Massif, according to which both, the high-*P*, high-*T* formation stage and the subsequent exhumation to mid-crustal levels, takes place in the presence of a partial melt. However, the modal amounts of melt observed in the experiments are generally much higher than those modelled by Roberts and Finger (1997) and the calculations presented above. Although the shift in the liquidus curves of peraluminous melts to lower temperatures when compared to the haplogranitic system allows the generation of larger amounts of melt (Johannes and Holtz, 1996) but the presence or absence of melt during peak *P-T* conditions in these granulites is still controversially discussed. Kotková (2007) states that it is agreed that granulite formation in the Bohemian Massif involved some degree of melting but the extent of melting and its timing in relation to the granulite *P-T* path are still under debate. While some authors (e.g. Vrána and Jakeš, 1982; Vrána, 1989; Jakeš, 1997; Kotková and Harley, 1999) suggested that the granulites represent rocks crystallized from high-pressure leucogranitic (or syenitic) magmas formed during the Variscan subduction, others favour

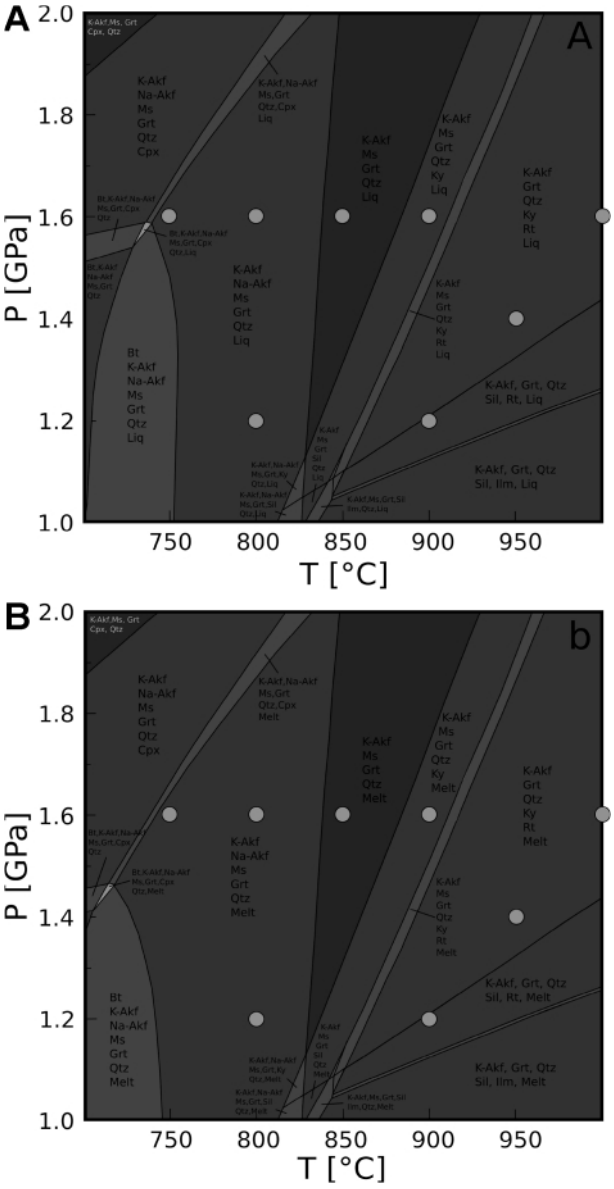

Figure 6: Pseudosections calculated with PERPLEX; (A) calculation using the muscovite activity model of Coggon and Holland (2002) and the extension of Azanneau et al. (2010) and the biotite activity model of White et al. (2007); (B) calculation using the muscovite activity model of Coggon and Holland (2002) and the extension of Azanneau et al. (2010) together with the biotite activity model of Tajcmanova et al. (2009). The white circles indicate the *P-T* conditions of the experiments of Tropper et al. (2005).

restricted partial melting at peak P-T conditions with possibly more significant melting at medium P along the decompressional path (Roberts and Finger, 1997; Janoušek et al., 2004; Tropper et al., 2005). White et al. (2011) discuss the discrepancy between observed and calculated amounts of melt during granulite genesis. Melting experiments dealing with natural rock systems such as the experiments of Tropper et al. (2005) cover a temperature range from fluid-absent subsolidus conditions at ca. 750°C to 1000°C and several studies have shown that over much of this range, the assemblages produced in typical metapelites and metagreywackes contain melt volumes in excess of 15 to 20 vol.%, and at the highest temperatures melt volumes of 50 vol.% or more can occur. In these fluid-absent studies fast and significant overstepping of the melting reactions may be particularly important to consider because in the subsolidus assemblage there is no fluid to facilitate diffusion between crystals and promote equilibration and hence it must be assumed that the high-degree of melting represents an experimental artefact. This experimental observation is in stark contrast to natural granulites since they do not follow such an evolution and efficient deformation-driven melt loss produces a residual chemistry and also preserves the high-temperature assemblage. Therefore while such experiments as carried out by Tropper et al. (2005) have relevance for identifying the initial fluid-absent melting reactions by which granulites melted they do not mimic the melting behaviour of such granulites.

Thermodynamic implications for the crystallization of accessory phases: Although the experimental investigations of Tropper et al. (2005) and theoretical calculations in this paper reproduce the main mineral assemblage garnet + 2 feldspars + quartz ± biotite observed in natural high-*P*/high-*T* granulites well the experiments indicated that it may be possible that some of the phases previously considered as belonging to the peak-*P*-*T* paragenesis may actually have formed during late-stage medium-pressure conditions. For instance, considering the peraluminous compositions of the experimentally produced melts and the trace amounts of kyanite present in the 1000°C/1.6 GPa and 950°C/1.4 GPa experiments, they argued it would be reasonable to assume that the kyanite of the South Bohemian granulites is not a phase formed under peak-*P*-*T* conditions but during uplift and decompression from a peraluminous melt. On the other hand the calculations of this study showed that kyanite is thermodynamically stable at almost all *P*-*T* conditions investigated. Concerning the presence of Ti-bearing phases the experiments by Tropper et al. (2005) contained very little rutile and significant TiO_2 contents in garnets. This could imply that the experiments are not rutile-saturated at high temperatures but have the entire TiO_2 partitioned between garnet and melt. On the other hand most of the granulites in the Southern Bohemian Massif have large accessory rutile crystals with sizes up to 0.2-1 mm and Tropper et al. (2005) argued that in the felsic granulite types rutile may thus not belong to the peak *P*-*T* paragenesis but formed along the cooling path at medium pressures, in the presence of melt. While these arguments might hold true for individual granulites thermodynamic calculations carried out in this study have shown that rutile is thermodynamically perfectly stable at these high-*P*/high-*T* conditions. Calculations with THERIAK-DOMINO have shown that rutile is stable at 850-1000°C/1.6 GPa and ilmenite is the stable Ti-phase under all other conditions. Calculations with PERPLEX have shown that rutile is stable under all *P*-*T* conditions considered. This clearly shows that one has to be extremely careful (small rutile or kyanite needles might have been overlooked due to their low abundance) in identifying minor and accessory phases in experimental run products and that thermodynamic calculations provide a reliable guidance which accessory phases are indeed stable at peak *P*-*T* conditions.

7. Conclusions

In order to compare the experimental results with thermodynamic predictions pseudosections with the programs THERIAK-DOMINO (De Capitani and Petrakakis, 2010) and PERPLEX (Connolly and Petrini, 2002) and the updated database of Holland and Powell (1998) were calculated. Despite using different activity models both programs yielded calculated phase relations and modes that are generally in good agreement with the experimental results and hence in further consequence with the naturally observed mineral assemblages in these high-*P*/high-*T* granulites. The main major discrepancies though lie in the stability of biotite, which is underestimated in the calculations using both programs (prediction is ca. 50-100°C lower at 1.6 and 1.2 GPa) and the amount of calculated vs. observed melt. Electron microprobe analyses showed that biotite contains up to 5 wt.% TiO_2 and 2 wt.% F. Although Ti contents can be considered empirically in Ti-biotite activity models (White et al., 2007; Tajcmanová et al., 2009) no biotite activity model involving F yet exists. Thus the low F content of the starting material of 1000 ppm therefore significantly perturbs the calculated phase relations involving biotite and one has to be cautious when calculating accurate biotite phase relations involving F in granulite-facies metamorphic rocks. The discrepancy concerning the modal amounts of melt most likely represents a lack of equilibration in the subsolidus stage of the experiments due to lack of fluid and the fast, large overstepping of melting reactions in the course of the experiments (see White et al., 2011). Nonetheless these experiments provide a reliable guidance concerning the nature of the melt-forming mineral reactions occurring in granulites at high-*P*/high-*T*. The combination of experimental investigations and thermodynamic calculations as shown in this study helps not only to constrain possible equilibrium assemblages but also helps to identify certain non-equilibrium features otherwise not detected anymore in natural granulites. The ultimate goal in constraining the metamorphic evolution of these high-*P*/high-*T* granulites is to reconcile data from experimental-thermodynamic investigations with natural field- and petrographic observations. Only this comprehensive approach will then allow to draw firm conclusions about the evolution of these highly un-

usual rock types and their implication for Variscan subduction zone geodynamics.

Acknowledgements

The authors want to thank Rainer Abart for his constructive review of the paper and Ralf Schuster for his editorial handling.

References

Auzanneau, E., Schmidt, M.W., Vielzeuf, D. and Connolly, J.A. D., 2010. Titanium in phengite: a geobarometer for high temperature eclogites. Contributions to Mineralogy and Petrology, 159, 1-24. http://dx.doi.org/10.1007/s00410-009-0412-7

Baldwin J.A., Powell, R., Brown, M., Moraes, R and Fuck, R. A., 2005. Modelling of mineral equilibria in ultrahigh-temperature metamorphic rocks from the Anapolis–Itaucu Complex, central Brazil. Journal of Metamorphic Geology, 23, 511-531. http://dx.doi.org/10.1111/j.1525-1314.2005.00591.x

Benisek, A,, Dachs, E. and Kroll, H., 2010. A ternary feldspar-mixing model based on calorimetric data: development and application. Contributions to Mineralogy and Petrology, 160, 327-337. http://dx.doi.org/10.1007/s00410-009-0480-8

Benisek, A., Kroll, H. and Cemic, L., 2004. New developments in two-feldspar thermometry. American Mineralogist, 89, 1496-1504.

Chatterjee, N.D. and Froese, E.F., 1975. A thermodynamic study of the pseudobinary to muscovite-paragonite in the system $KAlSi_3O_8$-$NaAlSi_3O_8$-Al_2O_3-SiO_2-H_2O. American Mineralogist, 60, 985-993.

Coggon, R. and Holland, T.J.B., 2002. Mixing properties of phengitic micas and revised garnet-phengite thermobarometers. Journal of Metamorphic Geology, 20, 683-696. http://dx.doi.org/10.1046/j.1525-1314.2002.00395.x

Connolly, J.A.D. and Petrini, K., 2002. An automated strategy for calculation of phase diagram sections and retrieval of rock properties as a function of physical conditions. Journal of Metamorphic Geology, 20, 697-708. http://dx.doi.org/10.1046/j.1525-1314.2002.00398.x

Cooke, R. A., 2000. High pressure/temperature metamorphism in the St.Leonhard Granulite Massif, Austria: evidence from intermediate pyroxene-bearing granulites. International Journal of Earth Sciences, 89, 631-651. http://dx.doi.org/10.1007/s005310000123

De Capitani, C. and Petrakakis, K., 2010. The computation of equilibrium assemblage diagrams with Theriak/Domino software. American Mineralogist, 95, 1006-1016. http://dx.doi.org/10.2138/am.2010.3354

Dooley, D.F. and Patiño Douce, A., 1996. Fluid-absent melting of F-rich phologipte + rutile + quartz. American Mineralogist, 81, 202-212.

Fiala, J., Matéjovská, O. and Vanková, V., 1987. Moldanubian granulites: source material and petrogenetic considerations. Neues Jahrbuch für Mineralogie Abhandlungen, 157, 133-165.

Finger, F., Cooke, R., Janoušek, V, Konzett, J., Pin, C., Roberts, M. P. and Tropper, P., 2003. The petrogenesis of the South Bohemian granulites: Highlighting the magmatic side of the story. Journal of the Czech Geological Society, 48/1-2, 44-45.

Franek, J., Schulmann, K. and Lexa, O., 2011. Origin of felsic granulite microstructure by heterogeneous decomposition of alkali feldspar and extreme weakening of orogenic lower crust during the Variscan orogeny. Journal of Metamorphic Geology, 29, 103-130. http://dx.doi.org/10.1111/j.1525-1314.2010.00911.x

Grant, J.A., 2009. Thermocalc and experimental modelling of melting of pelite, Morton Pass, Wyoming. Journal of Metamorphic Geology, 27, 571-578. http://dx.doi.org/10.1111/j.1525-1314.2009.00846.x

Grant, J. A., 1985. Phase equilibria in partial melting of pelitic rocks. In: Ashowrth, J. R. (ed) Migmatites. Blackie, Glasgow, pp 86-144.

Guy, A., Edel, J.B., Schulmann, K., Tomek, C. and Lexa, O., 2010. A geophysical model of the Variscan orogenic root (Bohemian Massif): Implications for modern collisional orogens. Lithos, 124, 144-157. http://dx.doi.org/10.1016/j.lithos.2010.08.008

Holland, T. J. B. and Powell, R., 1998. An internally-consistent thermodynamic data set for phases of petrological interest. Journal of Metamorphic Geology, 8, 89-124. http://dx.doi.org/10.1111/j.1525-1314.1990.tb00458.x

Holland, T.J.B. and Powell, R., 2001. Calculation of phase relations involving haplogranitic melts using an internally consistent thermodynamic dataset. Journal of Petrology, 42, 673-683. http://dx.doi.org/10.1093/petrology/42.4.673

Holland, T.J.B. and Powell, R., 2003. Activity-composition relations for phases in petrological calculations: an asymmetric multicomponent formulation. Contributions to Mineralogy and Petrology, 145, 492-501. http://dx.doi.org/10.1007/s00410-003-0464-z

Jakeš, P., 1997. Melting in high-P region – case of Bohemian granulites. Acta Universitatis Carolinae, Geologica, 41, 113-125.

Janoušek, V. and Holub, F.V., 2007. The causal link between HP–HT metamorphism and ultrapotassic magmatism in collisional orogens: case study from the Moldanubian Zone of the Bohemian Massif. Proceedings of the Geologists Association, 118, 75-86. http://dx.doi.org/10.1016/S0016-7878(07)80049-6

Janoušek, V., Gerdes, A. and Vraná, S., 2006. Low-pressure granulites of the Lisov Massif, Southern Bohemia: visean metamorphism of Late Devonian plutonic arc rocks. Journal of Petrology, 47, 705-744.

Janoušek, V., Finger, F., Roberts, M., Fryda, J., Pin, C. and Dolejš, D., 2004. Deciphering petrogenesis of deeply buried granites: whole-rock geochemical constraints on the origin of

largely undepleted felsic granulites from the Moldanubian Zone of the Bohemian Massif. Transactions of the Royal Society of Edinburgh, 95, 141-159. http://dx.doi.org/10.1017/S0263593304000148

Johannes, W. and Holtz, F., 1996. Petrogenesis and Experimental Petrology of Granitic Rocks. Springer Verlag, Berlin, 335 p.

Johnson, T.E., White, R.W. and Powell, R., 2008. Partial melting of metagreywacke: a calculated mineral equilibria study. Journal of Metamorphic Geology, 26, 837-853. http://dx.doi.org/10.1111/j.1525-1314.2008.00790.x

Kotková, J. and Harley, S.L., 1999. Formation and evolution of high-pressure leucogranulites; experimental constraints and unresolved issues. in „Crust melting in nature and experiment“ M. G. Brown and Kotková (eds.) Phys. Chem. Earth Part A: Solid Earth and Geodesy, 24, 299-304.

Kotková, J., 2007. High-pressure granulites of the Bohemian Massif: recent advances and open questions. Journal of Geosciences, 52, 45-71.

Kroll, H., Evangelakakis, C. and Voll, G., 1993. Two-feldspar geothermometry: a review and revision for slowly cooled rocks. Contributions to Mineralogy and Petrology, 114, 510-518. http://dx.doi.org/10.1007/BF00321755

Lexa, O., Schulmann, K., Janoušek, V., Stípská, P., Guy, A. and Racek, M., 2011. Heat sources and trigger mechanisms of exhumation of HP granulites in Variscan orogenic root. Journal of Metamorphic Geology, 29, 79-102. http://dx.doi.org/10.1111/j.1525-1314.2010.00906.x

Monier, G. and Robert, J.L., 1986. Muscovite solid solutions in the system K_2O-MgO-FeO-Al_2O_3-SiO_2-H_2O: an experimental study at 2 kbar P_{H2O} and comparison with natural Li-free white micas. Mineralogical Magazine, 50, 257-266. http://dx.doi.org/10.1180/minmag.1986.050.356.08

Munoz, J.L., and Ludington, S., 1974. F1uorine-hydroxyl exchange in biotite. American Journal Science, 274, 396-413. http://dx.doi.org/10.2475/ajs.274.4.396

Munoz, J.L., and Ludington, S., 1977. Fluorine-hydroxyel exchange in synthetic muscovite and its application to muscovite-biotite assemblages. American Mineralogist, 62, 304-308.

Patiño Douce, A.E., 1993. Titanium substitution in biotite: An empirical model with applications to thermometry, O, and H_2O barometries, and consequences for biotite stability. Chemical Geology, 108, 133-162. http://dx.doi.org/10.1016/0009-2541(93)90321-9

Peterson, J.W., Chacko, T., and Kuehner, S.M., 1991. The effects offluorine on the vapor-absent melting of phlogopite + quartz: Implications for deep-crustal processes. American Mineralogist, 76, 470-476.

Roberts, M.P. and Finger, F., 1997. Do U-Pb zircon ages from granulites reflect peak metamorphic conditions?, Geology, 25, 319-322. http://dx.doi.org/10.1130/0091-7613(1997)025<0319:DUPZAF>2.3.CO;2

Schulmann, K., Lexa, O. and Stípská, P., 2008. Vertical extrusion and horizontal channel flow of orogenic lowercrust: key exhumation mechanisms in large hot orogens? Journal of Metamorphic Geology, 26, 273–297. http://dx.doi.org/10.1111/j.1525-1314.2007.00755.x

Schulmann, K., Kroener, A. and Hegner, E., 2005. Chronological constraints on the pre-orogenic history, burial and exhumation of deepseated rocks along the eastern margin of Variscan orogen, Bohemian Massif, Czech Republic. American Journal of Science, 305, 407-448. http://dx.doi.org/10.2475/ajs.305.5.407

Stípská, P. and Powell, R., 2005. Does ternary feldspar constrain the metamorphic conditions of high-grade meta-igneous rocks? Evidence from orthopyroxene granulites, Bohemian Massif. Journal of Metamorphic Geology, 23, 627-647. http://dx.doi.org/10.1111/j.1525-1314.2005.00600.x

Stípská, P., Powell, R., White, R.W. and Baldwin, J.A., 2010. Using calculated chemical potential relationships to account for coronas around kyanite: an example from the Bohemian Massif. Journal of Metamorphic Geology, 28, 97-116. http://dx.doi.org/10.1111/j.1525-1314.2009.00857.x

Tajcmanová, L., Soejono, I., Konopásek, J., Košler, J. and Kloetzli, U., 2010. Structural position of high-pressure felsic to intermediate granulites from NE Moldanubian zone (Bohemian Massif). Journal of the Geological Society, London, 167, 329-345. http://dx.doi.org/10.1144/0016-76492009-086

Tajcmanová, L., Connolly, J.A.D. and Cesare, B., 2009. A thermodynamic model for titanium and ferric iron solution in biotite. Journal of Metamorphic Geology, 27, 153-165. http://dx.doi.org/10.1111/j.1525-1314.2009.00812.x

Tajcmanová L., Konopásek, J. and Schulmann, K., 2006. Thermal evolution of the orogenic lower crust during exhumation within a thickened Moldanubian root of the Variscan belt of Central Europe. Journal of Metamorphic Geology, 24, 119-134. http://dx.doi.org/10.1111/j.1525-1314.2006.00629.x

Tropper, P., Konzett, J. and Finger, F., 2005. Experimental constraints on the formation of high-P/high-T granulites in the Southern Bohemian Massif. European Journal of Mineralogy, 17, 343-356. http://dx.doi.org/10.1127/0935-1221/2005/0017-0343

Tonnes, R.G., Edgar, A.D., and Arima, M., 1985. A high pressure-high temperature study of Ti02 solubility in Mg-rich phlogopites: Implication to phlogopite chemistry. Geochimica et Cosmochimica Acta, 49, 2323-2329. http://dx.doi.org/10.1016/0016-7037(85)90232-7

Valley, J.W., Petersen, E.U., Essene, E.J., and Bowman, J.R., 1982. F1uorphlogopite and fluortremolite in Adirondack marbles and calculated C-O-H-F fluid compositions. American Mineralogist, 67, 545-557.

Vielzeuf, D. and Holloway, J.R., 1988. Experimental determination of the fluid-absent melting relations in the pelitic system: consequences for crustal differentiation. Contributions to Mineralogy and Petrology, 98, 257-276. http://dx.doi.org/10.1007/BF00375178

Vielzeuf, D. and Montel, J.M., 1994. Partial melting of metagreywackes. I. Fluid-absent experiments and phase relationships. Contributions to Mineralogy and Petrology, 117, 375-393. http://dx.doi.org/10.1007/BF00307272

Vielzeuf, D. and Schmidt, M.W., 2001. Melting relations in hydrous systems revisited: application to metapelites, metagreywackes and metabasalts. Contributions to Mineralogy and Petrology, 141, 251-267. http://dx.doi.org/10.1007/s004100100237

Vrána, S., 1989. Perpotassic granulites from southern Bohemia: a new rock-type derived from partial melting of crustal rocks under upper mantle conditions. Contributions to Mineralogy and Petrology, 103, 510-522. http://dx.doi.org/10.1007/BF01041756

Vrána, S. and Jakeš, P., 1982. Orthopyroxene and two-pyroxene granulites from a segment of charnockitic crust in southern Bohemia. Bulletin of the Czech Geological Survey, 57, 129-143.

White, R.W., Stevens, G. and Johnson, T.E., 2011. Is the crucible reproducible? Reconciling melting experiments with thermodynamic calculations. Elements, 7, 241-246. http://dx.doi.org/10.2113/gselements.7.4.241

White, R.W., Powell, R. and Holland, T.J.B., 2007. Progress relating to calculation of partial melting equilibria for metapelites. Journal of Metamorphic Geology, 25, 511-527. http://dx.doi.org/10.1111/j.1525-1314.2007.00711.x

White, R.W., Powell, R. and Holland, T.J.B., 2001. Calculation of partial melting equilibria in the system Na_2O–CaO–K_2O–FeO–MgO–Al_2O_3–SiO_2–H_2O (NCKFMASH). Journal of Metamorphic Geology, 19, 139-153. http://dx.doi.org/10.1046/j.0263-4929.2000.00303.x

Whitney, D.L. and Evans, B.W., 2010. Abbreviations for names of rock-forming minerals. American Mineralogist, 95, 185-187. http://dx.doi.org/10.2138/am.2010.3371

Received: 2 April 2014
Accepted: 23 September 2014

Peter TROPPER[1)*)] & Christoph HAUZENBERGER[2)]

[1)] Institute of Mineralogy and Petrography, University of Innsbruck, A-6020 Innsbruck, Austria;

[2)] Institute of Earth Sciences, University of Graz, 8010 Graz, Austria;

[*)] Corresponding author, peter.tropper@uibk.ac.at